Spring 5-2020

Direct Evidence of Missing mEPSPs Using Ca2-Sensor Imaging

Petar Gajic

Direct Evidence of Missing mEPSPs Using Ca^{2}-Sensor Imaging

An honors thesis presented to the
Department of Biology,
University at Albany, State University of New York
in partial fulfillment of the requirements
for graduation with Honors in Biology
and
graduation from The Honors College

Petar Gajic

Research Advisor: Gregory Lnenicka, Ph.D.
Second Reader: Ben Szaro, Ph.D.

May 2020

Abstract

Following an action potential in the presynaptic neuron there is evoked release of neurotransmitter into the synapse which activates ionotropic transmembrane receptors on the postsynaptic membrane that cause depolarizations in voltage that get recorded as excitatory postsynaptic potentials (EPSPs). In the absence of an action potential there is spontaneous release of neurotransmitter that postsynaptically gets recorded as miniature excitatory postsynaptic potentials (mEPSPs). According to the quantal hypothesis, postulated by Bernard Katz, the mEPSPs are all-or-none changes in potential caused by a single quantum of neurotransmitter, which when added up create EPSPs. Following studies have found that these two modes of vesicle release have differences in molecular mechanisms, vesicle recycling, and extracellular conditions of operation. Spontaneous release by itself is sufficient to maintain synaptic homeostasis and is involved in long-term potentiation. New data from our lab suggests that mEPSP frequency depresses after sustained stimulation of the presynaptic cell suggesting some feedback mechanism coming from the postsynaptic cell. In this study, following experimental observation that optical frequency from postsynaptic calcium sensor (GCaMP6) activation does not correlate with mEPSP frequency, we looked at what we call missing minis. Simultaneously recording optical and electrophysiological data we have found that certain fluorescence GCaMP6 flashes coming from glutamate receptor activation do not coincide with electrophysiological mEPSP events.

Acknowledgements

First, I would like to thank Andrew Powers, a doctoral student in our laboratory for help throughout my time there. He has taught me a lot of important skills that I have used in my work such as the handling of animals and the data analysis.

Second, I would like to thank Professor Szaro for agreeing to be the second reader of my thesis, and for the after-class discussions we had on life and neuroscience.

Finally, I thank Professor Lnenicka for allowing a naive sophomore into his lab. Foolheartedly I thought that knowing a little chemistry and biology would help me understand what electrophysiology was. Luckily, the Professor helped me manage my way through this field, and as time went on, I got to appreciate, understand, and love electrophysiology. Thank you again Professor for this opportunity and your guidance. Viewing basic science research and courses as the bedrock of my future career.

List of Figures

List of Tables

Table of Contents

Introduction

The science of electrophysiology began with experiments performed by Luigi Galvani on muscle contraction in the frog muscle, which he believed originated from electricity originating in the animal itself. Galvani found that discharging a Leyden Jar could produce contraction of frog leg muscles, and hypothesized that there could be an internal electrical force that causes the muscles to contract under normal conditions and that the muscles accumulate electricity not nerves due to their relative bigger size. He proposed that the muscle fibers in these muscles have duplex (positive and negative) electricity (Galvani, 1791, 1937; Piccolino, 1998)

Following this period and before the work of Hodgkin, Huxley, Fatt, and Katz, there was work by various scientists on the electrical nature of the cell. Scientists such as Matteucci found that muscle fibers themselves have an intrinsic biological origin of electricity (Matteucci, 1844; Piccolino, 1998). These experiments were confirmed by the German scientist du Bois-Reymond who using a galvanometer managed to record a negative potential on the outer muscle membrane when compared to more distant (inactive) parts with respect to the muscle and nerve (du Bois-Reymond, 1884; Piccolino, 1998). The next notable German scientist was Hermann von Helmholtz who managed to measure the propagation speed of the nervous impulse (Helmholtz, 1850, 1852; Piccolino, 1998). After him, Julius Bernstein looking at neurons hypothesized the theory of membrane polarization in which the inside of the cell is more negative with respect to the outside, and that during excitation electrical resistance decreases (Bernstein, 1912; Piccolino, 1998)

Modern electrophysiology came into being with the experiments of Hodgkin and Huxley who discovered that the cause of electrical propagation (action potential) down the squid giant axon was the movement of sodium ions across the cell membrane to the inside of the cell, and the movement of potassium ions across the membrane to the outside of the cell (Piccolino, 1998;

Schwiening, 2012). Receiving a Nobel Prize in Medicine and Physiology in 1963 their work was soon followed up by another groundbreaking neurobiological discovery that was made by the 1970 Nobel Prize in Medicine and Physiology recipient Bernard Katz who discovered that when the action potential reaches the motor endplate acetylcholine is released in packets of vesicles that are quantized (Augustine & Kasai, 2007; Del Castillo & Katz, 1954b; Fatt & Katz, 1952; Piccolino, 1998). Katz further observed that a resting motor endplate of a muscle fiber produced spontaneous electrical discharges, which he called the miniature end-plate potential (miniEPP) (Fatt & Katz, 1952). When recording the values of the amplitude of the miniature end-plate potentials the amplitude remained fairly constant, while the frequency was subject to change. He found that these miniEPPs arise post-synaptically at the end-plate and their amplitudes were about 1/100 the size of regular end-plate potentials (Fatt & Katz, 1952). In the follow-up study by Katz, he proposed that these miniEPPs were caused by quantum packets of neurotransmitter, which added together to create the end-plate potentials (Del Castillo & Katz, 1954b). This stems from the observation that reducing the Ca2+ concentration reduced the size of the EPP to that of the miniEPP (Fatt & Katz, 1952).

Following this study, Katz formulated the quantal hypothesis. Katz' postulate was that when reducing Ca^{2+} concentration and increasing Mg^{2+} concentration transmitter release is decreased to a single quantum and the EPP becomes the same size as the miniEPP. If Ca2+ concentration was increased, the size of the EPP would be larger due to increases probability of spontaneous release and the release of more quanta of transmitter. Thus suggesting that these miniEPPs are all-or-none smallest units of potential change that make up EPPs (Del Castillo & Katz, 1954b). It was observed that an increase in temperature, or the osmolarity of the extracellular fluid by increasing concentration of NaCl or sucrose would increase the frequency of miniEPPs

(Fatt & Katz, 1952). Further studies in the changes of osmolarity used extracellular increases in ethanol and glycerol produced a transient increase in frequency that over time went down possibly due to these chemicals penetrating the membrane more rapidly than NaCl and Sucrose. They assumed that changes in osmolarity affected the presynaptic terminal and the release of quanta of transmitter producing the miniEPP (Furshpan, 1956). Further evidence that the miniEPPs were produced by the release of neurotransmitter came from studies of botulinum toxin, which acts at the neuromuscular junction (NMJ) to block the release of acetylcholine (Sellin, 1980). Botulinum toxin resulted in a decrease in the frequency of spontaneous miniEPPs leading to the complete cessation of miniEPPs but no change in the amplitude (Brooks, 1956). However, the EPPs were decreased in amplitude by the toxin (Brooks, 1956). What was also found to change the frequency of miniEPPs was the passing of both cathodic and anodic polarization using non-polarizable electrodes to pass direct current (dc) at the terminal end of the motor axon. Cathodic currents were found to increase the frequency of miniEPPs, while the anodic current producing no change in frequency until a threshold was reached and then would produce high-frequency bursts (Del Castillo & Katz, 1954a).

The quantal hypothesis for transmitter release first described at the vertebrate NMJ applies at all synapses. At most synapses, the evoked potentials are called excitatory post-synaptic potentials (EPSPs) the spontaneous potentials are referred to as miniature excitatory post-synaptic potentials (mEPSPs). According to the quantal hypothesis these mEPSPs have all-or-none nature and are the building blocks of EPSPs represented by the equation m=EPSP/mEPSP, where m represents the quantal content, or the number of vesicles released (Del Castillo & Katz, 1954b).

The place where the quanta of transmitter are released on the presynaptic neuron is called the active zone (Couteaux & Pecot-Dechavassine, 1970; Südhof, 2012). These active zones appear

as electron dense regions when viewed with electron microscopy (Walrond & Reese, 1985). They are the sites where synaptic vesicles dock and the Ca^{2+} channels are located (Harlow et al., 2001). These synaptic vesicles, which contain a quantum of transmitter, have varying diameters that range from 200A to 650A (De Robertis & Franchi, 1956). This release of vesicles is triggered by influx of Ca^{2+} through voltage-gated calcium channels in response to membrane depolarization produced by action potentials (Ramakrishnan et al., 2012). The fusion of synaptic vesicle to the presynaptic membrane and transmitter exocytosis involves tSNARE (soluble N-ethylmaleimide-sensitive fusion protein attachment protein receptors) proteins (Ramakrishnan et al., 2012). The mechanism of this release was looked at in a review for synchronous (after action potential), asynchronous (longer time period after the action potential or train of action potentials), and spontaneous release and it appears that they share key molecular mechanisms of release involving SNARE proteins synaptobrevin 2/VAMP2, SNAP-25, and syntaxin-1. However, spontaneous release appears to be Ca2+ independent in Drosophila (Kaeser & Regehr, 2014).

At the synaptic level it has been found that there are distinct synapses that favor one way of transmission either evoked or spontaneous. Presynaptic levels of Bruchpilot (brp) protein have been found to influence the release of vesicles, such that synapses that have higher levels of this protein favored evoked transmission, while synapses that have lower levels favor spontaneous release (Peled et at., 2014). This was discovered by visualizing transmitter release using GCaMP6 targeted to the postsynaptic membrane. GCaMP6 is a genetically encoded calcium sensor based on the green fluorescent protein (Cichon et al., 2020; Nakai et al., 2001), it consists of a circularly permuted green fluorescent protein (cpGFP), the calcium-binding protein calmodulin (CaM), and CaM-interacting M13 peptide (Chen et al., 2013). Calcium binds to the M13/CaM which induces a change in the GFP chromophore that creates fluorescence detectable by recording equipment

(Chen et al., 2013). The GCaMP6 version of the GCaMP family of proteins was found to produce the most sensitive and fastest Ca^{2+} binding (Reiff et al., 2005). Due its ability as a calcium sensor to produce a visual cue it has been used in detecting action potentials, spontaneous, and evoked release (Melom et al., 2013; Tian et al., 2005). The method of expression of GCaMP6 is through the Gal4/UAS-system (Brand & Perrimon, 1993; Reiff et al., 2005) in the cells of interest.

Recording action potentials, spontaneous, and evoked release is done using fluorescence microscopy, imaging a whole nerve terminal, and selecting regions of interest (ROI) (Leitz & Kavalali, 2014; Melom et al., 2013; Murthy et al., 1997). This is done by selecting for morphological (Peron et al., 2015a) or activity-based regions (Diego et al., 2013; Peron et al., 2015b). Using GCaMP imaging by selecting for regions of interest in the terminal it has been found that spontaneous and evoked release coincided or were separate from one another (Melom et al., 2013; Nakai et al., 2001). Recording spontaneous vesicle release using fluorescent microscopy techniques and mEPSPs using intracellular electrodes, researchers found that the appearance of a GCaMP flash would coincide with mEPSP elecrophysiological recordings (Melom et al., 2013). According to these studies the separate method of spontaneous and evoked release should be two different methods of synaptic communication in terms of activating different molecular mechanisms for vesicle release, different locations on the synapse they are released, and activating different receptors on the post-synaptic cell.

There are observed functions of spontaneous release in several animals. In the *Drosophila melanogaster* NMJ, mutations in the DGluIIA receptor decreased quantal size (mEPP amplitude) in the postsynaptic cell, which is compensated by an increase in quantal content. Indicating that the compensation uses some retrograde signal to induce a homeostatic change (Petersen et al., 1997). By blocking motoneuron activity and evoked release, researchers found that the

spontaneous release alone is sufficient in induction in synaptic homeostasis, indicating even small changes in postsynaptic excitability can induce presynaptic changes in vesicle release (Frank et al., 2006). In the CA1 pyramidal neurons, spontaneous vesicle release of glutamate has been found to act as a trophic factor and prevent loss of dendritic spines by acting on GluR1 AMPA receptors by maintaining them (McKinney et al., 1999), and that the diffusional movement of GluR1 is confined to restricted subregions on the postsynaptic membrane by spontaneous activity (Ehlers et al., 2007). Other studies found that through spontaneous glutamate release, protein synthesis in dendrites is affected through activation of NMDAR receptors, they function in terms whether a synapse will be strengthened, maintained, or eventually lost (Sutton et al., 2006). This effect on synaptic plasticity has been discovered in *Aplysia* in which it was reported that spontaneous release is a critical signal for the induction of long-term facilitation. The frequency and the amplitude of mEPSCs (or mEPSPs) increases with synaptic facilitation, with both long-term and intermediate effects (Jin et al., 2012).

The *Drosophila melanogaster* neuromuscular junction (NMJ) is a popular system for studying synaptic plasticity, allowing for good utilization of electrophysiological, genetic, and imaging techniques (Frank, 2014). At the Drosophila NMJ it has been found that voltage clamping muscle fibers 5 and 6 resulted in depression of mEPSP current 30 seconds post stimulation in HL3.1 (1.5mM Ca^{2+}) but not in HL3 (1mM Ca2+) indicating that increased [Ca2+] resulted in decreased frequency. The amplitudes in mEPSC for both solutions post-stimulation increased. When using buffers such as BAPTA increased the mEPSC frequency after stimulation (Powers et al., 2017). Unpublished data from our lab, using GCaMP6 calcium sensors, show that when recording the optical frequency 30sec post-stimulation and comparing it to the mEPSP frequency 30sec post-stimulation there is a discrepancy between the two recordings. The frequency of

GCaMP6 shows no decrease in frequency post-stimulation, while the mEPSP frequency shows a decrease post-stimulation indicating a presence of missing mEPSPs.

In this study we simultaneously recorded spontaneous GCaMP6 flashes along with miniature excitatory postsynaptic potentials at the *D. melanogaster* NMJ terminal. Instead of selecting for individual regions of interest along the active zones, as in the previously mentioned studies, we have selected the whole terminal. Recordings of the GCaMP6 fluorescent flashes when compared to the mEPSP data from the same animal, show that there are certain optical events that do not coincide with electrophysiological recordings. This indicates that there is activation of glutamate receptors without a corresponding change in potential.

Methods

Experimental Animal

Drosophila melanogaster was were raised in a Percival® Intellus incubator at 25°C in 12-hour light/ 12-hour dark environment on Jazz Fly Media. The two fly stocks raised were P{GAL4-Mef2.R} and P{how24B-GAL4} which would be the muscle driver, and P{UAS-GCaMP6} with the calcium sensor fluorescent protein. The P{UAS-GCaMP6} would be cleared of non-virgin adults from the vials. Following a time period from 4-8 hours after clearance female P{UAS-GCaMP6} virgin flies would be collected and put into separate Jazz Fly Media vials prior to doing a cross. Males from either P{GAL4-Mef2.R} or P{how24B-GAL4} would be collected. These would be put into separate Jazz Fly Media vials. These two muscle driver groups would be crossed with a minimum of 4 virgin female P{UAS-GCaMP6} flies. Ten days after the cross 3rd instar larvae that exhibit fluorescence under a fluorescent microscope would be selected for experimentation.

mEPSP electrophysiology recordings

Miniature excitatory post-synaptic potentials were recorded using sharp microelectrodes (15–25 MΩ filled with 3 M KCl) connected to an Axoclamp® 2A amplifier (Molecular Devices®, Sunnyvale, CA) in HL3 saline containing 1.0 mM Ca2+. The electrodes were inserted into 3rd instar larvae muscle fiber 4. The mEPSP recordings were collected using ClampFit® software. For the experiments that used both mEPSP recordings and fluorescence recordings both were performed simultaneously.

GCaMP6 fluorescence imaging

Following the cross of female P{UAS-GCaMP6} flies with either P{GAL4-Mef2.R} or P{how24B-GAL4} 3rd instar larvae offspring would exhibit fluorescence. Imaging was done on muscle fiber 4 which has both the Ib and Is terminal boutons (Atwood et al., 1993). Using a

fluorescence microscope and MetaFluor® as recording software images were taken for 1 minute at a frequency of 20Hz. Frequencies of mEPSP were taken in the 0-30 sec and 30-60 sec.

Selection of Boutons and Bottlenecks and measuring distance

For the GCaMP recordings MetaFluor® was used to select regions that are considered boutons with the same size and shape regions placed as a background. The pixel values of each image were recorded for 1 minute, saving the data in Microsoft Excel®. The imaging data was repeated, and the regions between the boutons were selected and named bottlenecks, saving the data in Microsoft Excel®. For both sets of data pixel values of boutons were subtracted from the background and converted into files for analysis in MiniAnalysis®. The peaks in the waveform data each represented a peak of GCaMP6 flashes. For the experiments that recorded mEPSP data, these methods were repeated. The distance of the whole terminal was taken in MetaMorph®. Measuring was calibrated in µm, and the distance for Ib was taken as well as distance for Is (n=1). To get the distance of the whole terminal Ib and Is were added together. The frequencies of GCaMP were taken in 0-30sec and 30-60sec and divided by the length of the Ib+Is length. The averages of mEPSP data was compared to these values by performing a t-test in SigmaPlot®.

Simultaneous mEPSP and imaging recordings

For this set of experiments the preparation of the 3rd instar larvae, the mEPSP recordings, and the GCaMP6 imaging data had the same setup. The recording for both electrophysiology and imaging had to start and the same time, this was achieved by setting up flashes of light in the microscope apparatus. This resulted in different analysis of the data. First by reducing the recording frequency of electrophysiology data to 1KHz. Then in SigmaPlot® the waveforms for both the electrophysiology and imaging were compared

Results

The structures that made the synaptic boutons visible when compared to the background were the subsynaptic reticulum of the *D. melanogaster* NMJ. Most of the fluorescence images that were recorded were that of the Ib boutons only, due to the difficulty of capturing both Ib and Is on the same image.

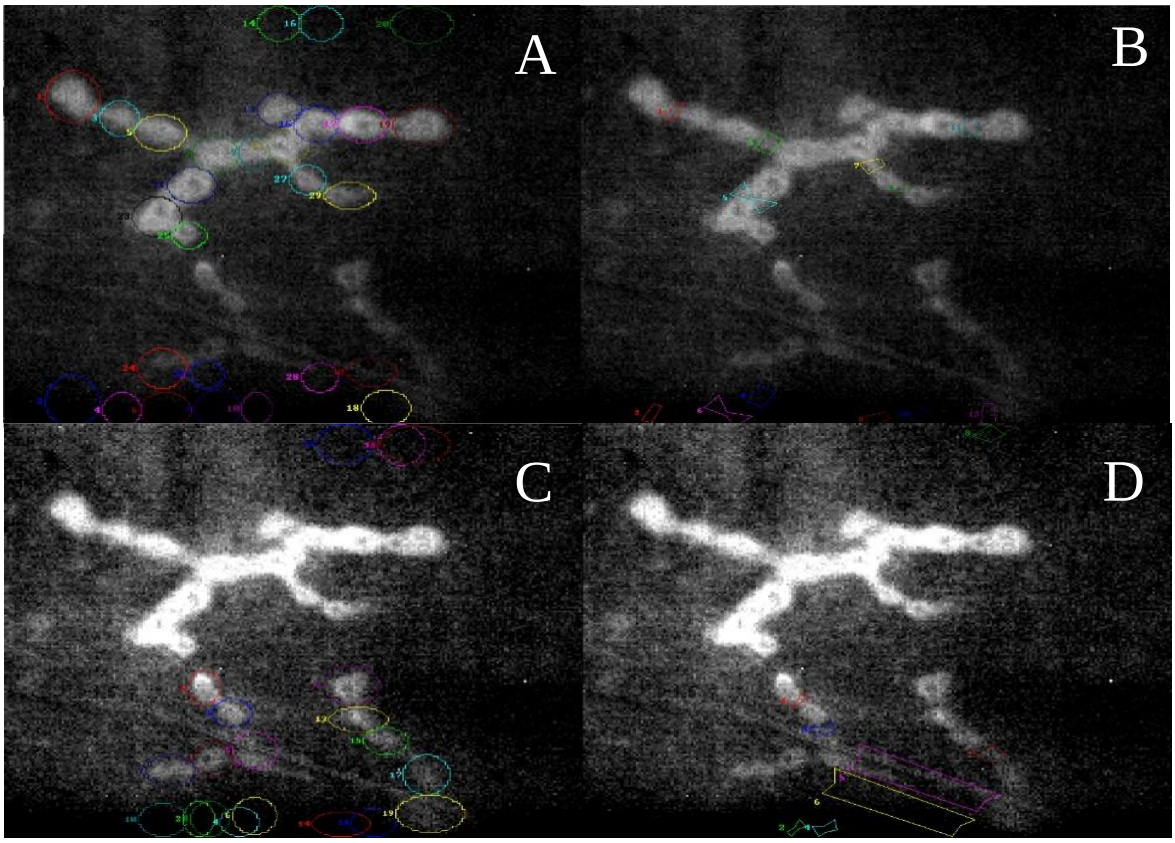

Figure 1. Shows the monochrome Ib and Is boutons on a single preparation.

(A) Shows the selection of ROIs for the Ib terminal boutons of the *D. melanogaster* NMJ. At the bottom of the image are the ROIs for the background that was subtracted from the boutons to obtain a pixel value. (B) Shows the bottleneck ROIs that were manually selected for between the bouton regions. (C) Shows the ROIs for the Is terminal boutons, with the background ROIs. (D) Shows the bottleneck ROIs between the boutons on the Is. The difference in light intensity coming from the Ib and Is is due to the density of SSR.

Following the recording of these images the data was taken into Excel® where the background values for fluorescence were subtracted from the values of boutons (Table 1.)

Time (ms)	R1 W1 Avg	R2 W1 Avg	R3 W1 Avg	R4 W1 Avg	R1-R2	R3-R4
0	3095.4	2630.25	3146.45	2608.17	465.15	538.28
50	3094.23	2631.95	3138.44	2613.16	462.28	525.28
100	3103.05	2637.85	3144.89	2611.72	465.2	533.17
150	3108.02	2633.47	3143.56	2620.65	474.55	522.91

Table 1 Bouton pixel values. Shows a part of the imaging data with the numbers representing the average pixel value of R1 (bouton 1 selection on figure 1), R2 (bouton 1 background), R3 (bouton selection 3), and R4 (background). The R1-R2 is the value of bouton selection 1 (R1) subtracted from the background pixel value (R2). The R3-R4 is the subtraction of bouton selection 3 (R3) to background 4 (R4).

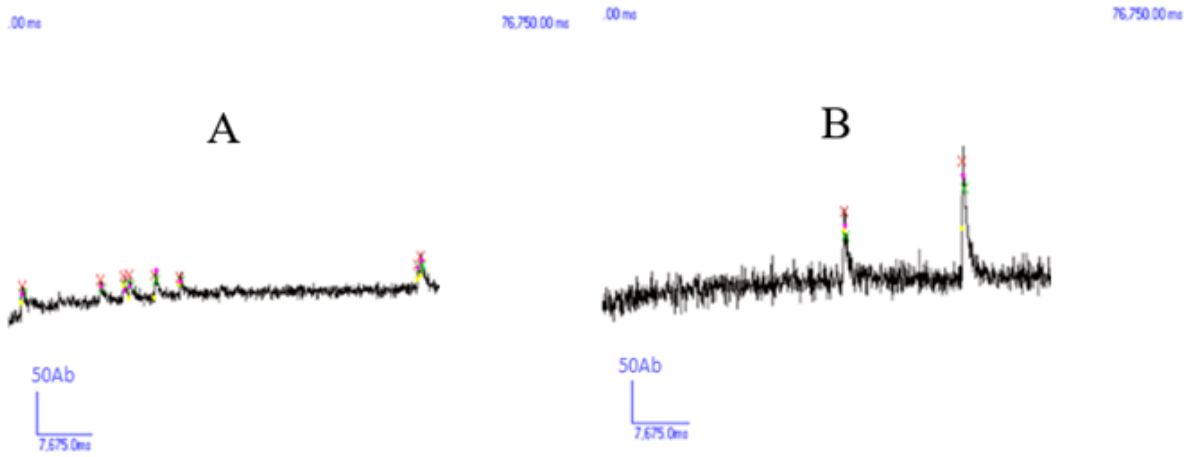

Figure 2 Shows the waveforms of GCaMP6 fluorescence pixel values. (A) shows bouton selection 19 waveform of Ib from the preparation above. There is a total of 6 fluorescence events that occurred during the 60 second recording time. (B) shows bottleneck selection 7 waveform of Ib from the preparation above. There is a total of 2 fluorescence events that occurred during the 60 second recording time.

The last two columns in Table 1 contain values that were represented individually as waveforms in MiniAnalysis® software, and the numbers of peaks that represented individual GCaMP6 fluorescence flashes were selected for. The selection method is detailed in Figure 2 which shows one bouton and one bottleneck waveform from the preparation mentioned above. These have differing amplitudes of GCaMP due to the average pixel values coming from the selection, the noise was higher usually in bottleneck selections, due to the small areas of selection and the movement coming from the preparation under the microscope. This error is negligible due

to the peaks themselves and their frequency being taken into account, not the amplitudes of GCaMP6 flashes. These waveforms were done for each of the selections above for both the bottlenecks and boutons, and the numbers of flashes taken in order to find the frequency of Ib (Table 2), and frequency of Is (Table 3). Frequency for entire terminal calculated as (total length of terminal/measured length of terminal) x frequency (Table 2 & 3).

Time (sec)	GCaMP events at boutons	GCaMP events at bottlenecks	frequency of GCaMP6 flashes (Hz)	Total frequency (Hz)
0-30	28	4	1.07	1.0667
30-60	24	5	0.97	0.9667

Table 2 Shows the total number of GCaMP6 events in the above preparation from both bottlenecks and boutons in the Ib. The number of events in 0-30sec, and 30-60sec. Frequency of events was calculated 32/30 (0-30), and 29/30 (30-60). This data comes from the recordings in Figure 1. Note the last two columns are the same since the measured and total length are equal (not the case in every preparation.

Time (sec)	GCaMP6 events at boutons	GCaMP6 events at bottlenecks	frequency of GCaMP6 flashes (Hz)	Total frequency (Hz)
0-30	25	1	0.87	0.87
30-60	30	3	1.1	1.1

Table 3. Shows the total number of GCaMP6 events in the above preparation from both bottlenecks and boutons in the Is. The number of events in 0-30sec, and 30-60sec. Frequency of events was calculated 32/30 (0-30), and 29/30 (30-60). This data comes from the recordings in Figure 1. Note the last two columns are the same since the measured and total length are equal (not the case in every preparation).

prep	1	2	3	4	5	6	7	8	9	10	11	12
0-30 freq	0.7667	1.0667	2.6667	0.8333	0.8667	1.9	0.4667	1.4	2.5	1.9	1.7	0.7667
30-60 freq	0.6	0.9667	2.0333	0.9	0.6333	1.4667	0.4333	1.5667	2.8333	1.2	1.6	0.3667
0-60 freq	0.68	1.02	2.35	0.8667	0.75	1.683	0.45	1.48	2.67	1.55	1.65	0.5667

Table 4. Shows the frequencies of all trials (n=12). These all represent Ib bouton frequencies. These experiments were repeated for the remaining preps to get the frequencies of GCaMP6 flashes. There was a total of n=12 preps (Table 4.). Most of these preps only had Ib. Trial 2 (above), was the sole Ib+Is.

.

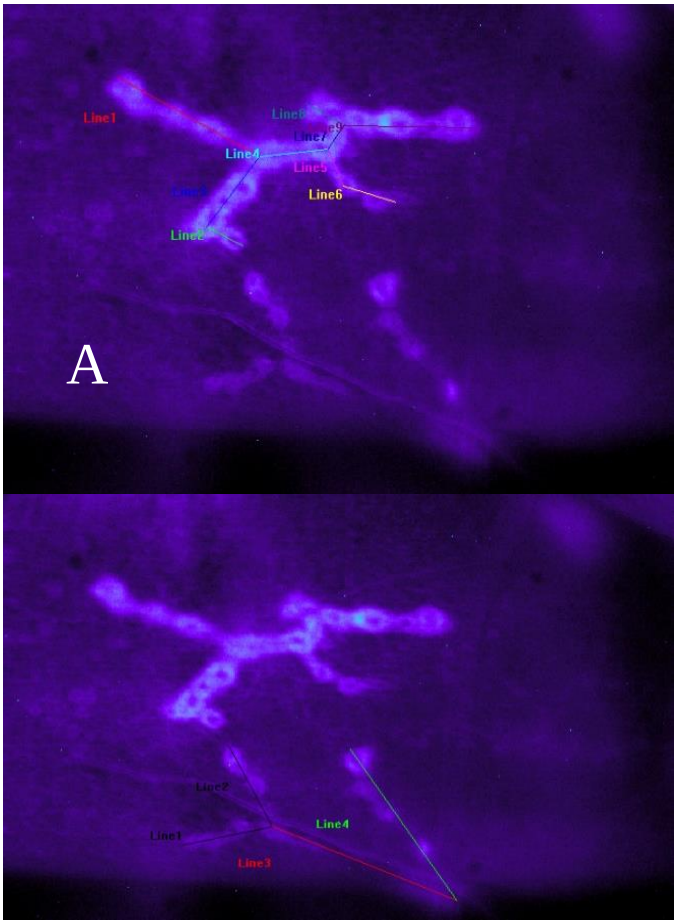

Figure 3 Shows the length measurements on prep 2 Ib and Is terminals. (A) Shows the measuring of Ib terminals using calibrated lines. The values obtained when these line distances were added together was 125.6676 µm. (B) Shows the measuring of Is terminals using calibrated lines. The size of the Is when the individual lines were added together was 114.9688 µm. These were performed in MetaMorph®.

line	IB (µm)	IS (µm)
1	30.4166	17.7589
2	8.11807	19.2645
3	16.4247	39.2928
4	12.9796	38.6526
5	7.65419	
6	10.4049	
7	5.91515	
8	8.21909	
9	25.5353	
totals	125.6676	114.9688

Table 5. Length measurements from prep 2.

Data from every preparation (Table 6) was analyzed as preparation 2 was. The numbers of GCaMP6 flashes for each preparation was taken and the frequencies were found (Table 6.B) as (number of flashes)/60sec. Since there was only one Is

terminal it was found in the same manner (Table 6.C). The length of the terminal containing the ROIs used to determine GCaMP6 flash frequency was measured and referred to as the "ROI terminal length" (Figure 3) (Table 6.D). When looking at the full chip for the entire terminal with there were regions that had no ROIs, these lengths were also measured and added to the numbers in Table 6D to obtain the "Total terminal lengths" (Table 6.E). Some had their full lengths measured the first time and were included as they were, example being preparation 2 which had both 125 microns for both lengths. The total frequency for the Ib was calculated as (Total terminal length/ROIterminal length) x Ib frequency (Table 6.F). The same was repeated for Is (Table 6.G). The total frequency of GCaMP6 flashes was taken as the sum of Is and Ib (Table 6.H). With this value we obtained a frequency of GCaMP6 flashes along the whole terminal for muscle fiber 4.

A-prep #	1	2	3	4	5	6	7	8	9	10	11	12
B-Ib frequency (0-60sec) (Hz)	0.6834	1.0167	2.35	0.8667	0.75	1.6834	0.45	1.4834	2.6667	1.55	1.65	0.5667
C-Is frequency (0-60sec) (Hz) (n=1)	0.98335	0.98335	0.98335	0.98335	0.98335	0.98335	0.98335	0.98335	0.98335	0.98335	0.98335	0.98335
D-ROIs terminal length (µm)	55.9284	125.6676	139.8551	88.9317	65.8931	111.3225	149.1043	83.5701	100.8848	79.2648	113.9392	59.7283
E-total terminal length (µm)	81.7714	125.6676	139.8551	165.011	124.596	111.3225	149.1043	83.5701	100.8848	79.2648	113.9392	59.7283
F-total IB frequency (Hz)	0.9991	1.0167	2.35	1.6081	1.4182	1.6834	0.45	1.4834	2.6667	1.55	1.65	0.5667
G-total IS frequency (Hz)	0.98335	0.98335	0.98335	0.98335	0.98335	0.98335	0.98335	0.98335	0.98335	0.98335	0.98335	0.98335
H-total frequency (Ib+Is) (Hz)	1.9824	2	3.3334	2.5914	2.4015	2.6667	1.4334	2.4667	3.65	2.5334	2.6334	1.55

Table 6. Shows the data from all the preparations, along with their frequency per Ib terminal (B), frequency per Is (C). The length of the terminals that had bouton and bottleneck selections (D). The length of the total terminal containing regions with no ROIs (E). Total GCaMP6 frequency for the whole length of the Ib terminal (F) and Is terminal (G). With the average total frequency of Ib + Is (H).

The average frequencies of GCaMP6 over the 60 second recording period (Table 6H), were compared to the averages of mEPSPs over the recoding period of 60 seconds. This was done statistically in a t-test in which the Two-tailed *p*-value = 0.00466. Showing that there is a

significant difference between these two groups. This provides evidence for missing mEPSP; i.e., there is transmitter release (GCaMP flashes) that do not result in a mEPSP.

Normality Test (Shapiro-Wilk) *Passed (P = 0.195)*

Equal Variance Test: *Passed (P = 0.073)*

Group Name	**N**	**Missing**	**Mean**	**Std Dev**	**SEM**
avgs	12	0	2.437	0.646	0.187
avgs	9	0	1.391	0.853	0.284

Difference 1.046

t = 3.205 with 19 degrees of freedom.

95 percent two-tailed confidence interval for difference of means: 0.363 to 1.729

Two-tailed P-value = 0.00466

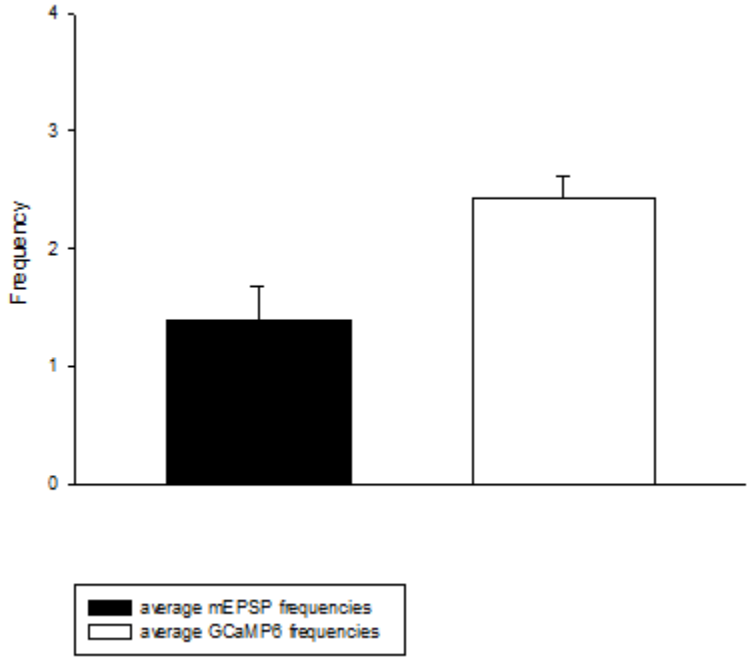

Figure 4. Shows the bar graph of the two average frequencies from Table 6. compared. The average frequencies of GCaMP6 (white bar) were higher than the average mEPSP frequencies (black bar).

To examine whether there were missing mEPSPs more directly, we simultaneously recorded the mEPSPs together with the GCaMP6 fluorescence. In this case, we could directly examine whether the GCaMP flash was always accompanied by a simultaneous mEPSP.

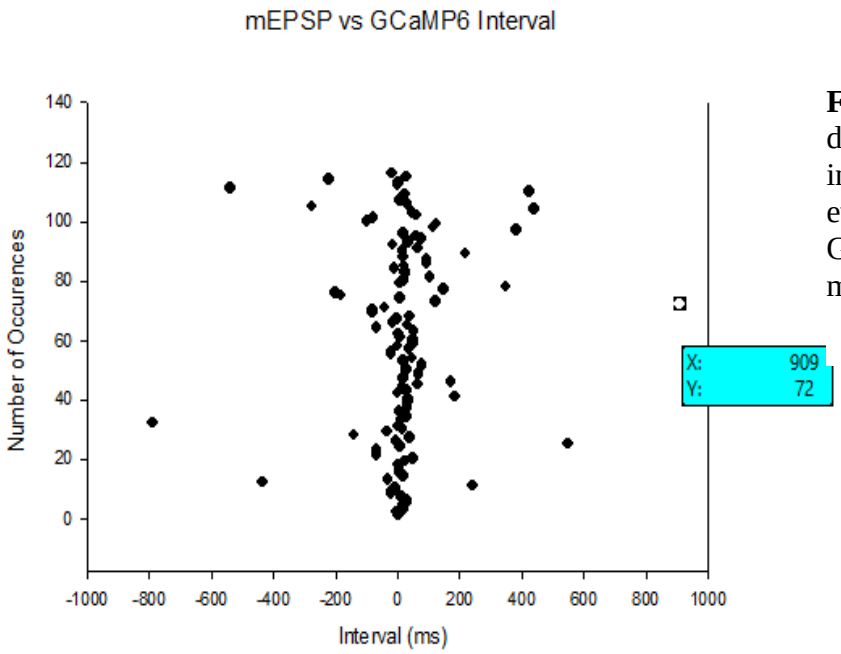

Figure 5. Shows a scatter plot of the differences in the time interval among the individual GCaMP6 flashes and mEPSP events. The highlighted dot represents a GCaMP6 flash without a corresponding mEPSP recording.

Scatter plot of the time difference interval between the GCaMP6 peak and the mEPSP peak was obtained by taking the time of the peak GCaMP6 and subtracting closest time of peaks of mEPSP (Figure 5). The values that are close to, or at the value of zero represent GCaMP6 fluorescent flashes that have a corresponding mEPSP recording. The longer intervals result from mEPSP produced by terminals regions that were not selected as ROIs and these GCaMP flashes did not produce a mEPSP. Note that the negative values represent a time of mEPSP occurrence that is before a GCaMP6 optical event, and the positive values represent a time of mEPSP occurrence that is after a GCaMP6 optical event (Figure 5). The highlighted value in Figure 5 has a interval difference of 909ms, which shows that there is no mEPSP recording for that GCaMP6 event. This is visualized as a waveform of this larvae mEPSP (Figure 6A) and compared to the GCaMP6 waveform from bouton selection 9 of this preparation (Figure 6A).

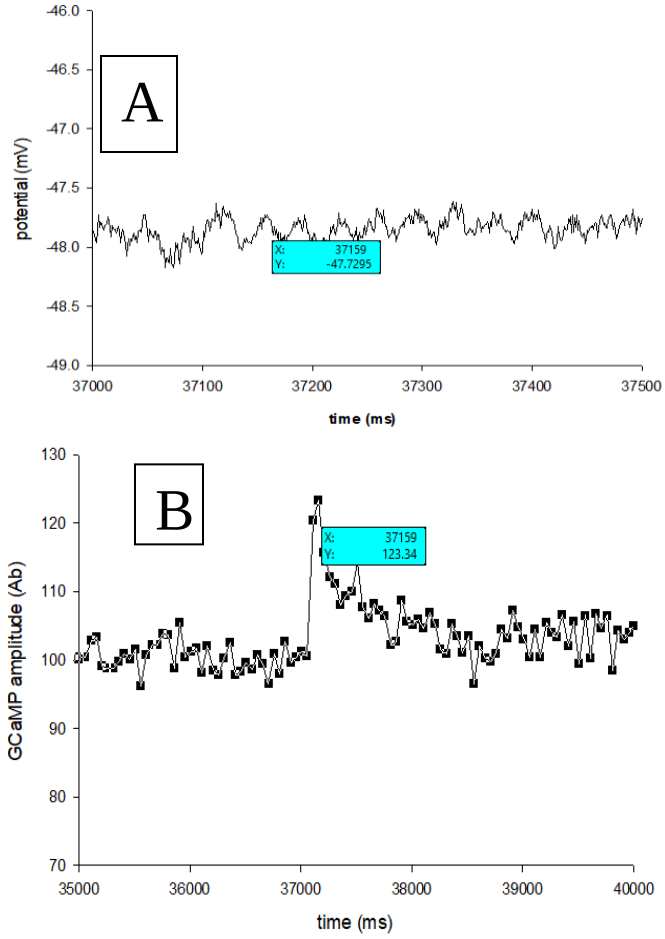

Figure 6. Shows the mEPSP and GCaMP6 waveforms from the same preparation. (A) Shows the mEPSP recordings with the X value of 37159ms highlighted. (B) Shows the GCaMP6 recording from bouton 9 with the X value of 37159ms highlighted. These x values represent the time course of the experiment. This figure indicates the missing miniature excitatory post synaptic potential. The activation of GluR on the post synaptic NMJ does not coincide with a mEPSP recording.

The events that were recorded also had values from GCaMP6 and mEPSP that overlapped as indicated in Figure 7.

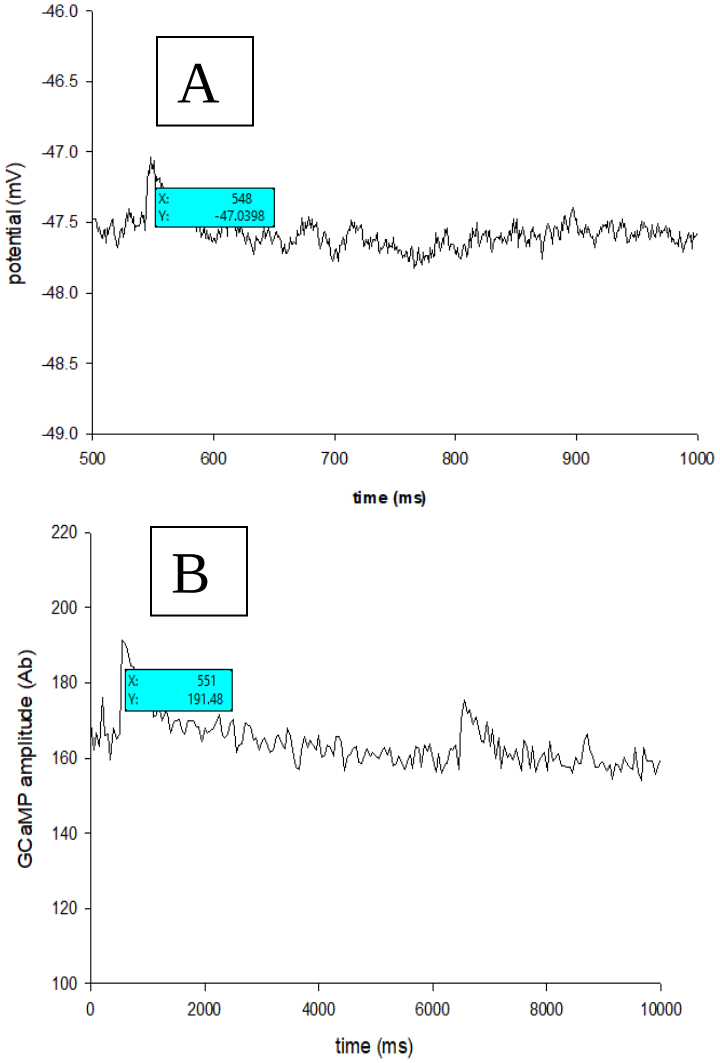

Figure 7. Shows the overlap of the events on the waveform for the GCaMP6 and mEPSP data. (A) Shows a peak at 548ms on the mEPSP data. (B) Shows a peak on 551ms on the GCaMP6 data. These two shows that following a GCaMP6 flash we do see a post synaptic depolarization that is recorded as a mEPSP. (C) Shows the scatter plot and the value that represents these two events with an interval difference of 3ms (x=3)

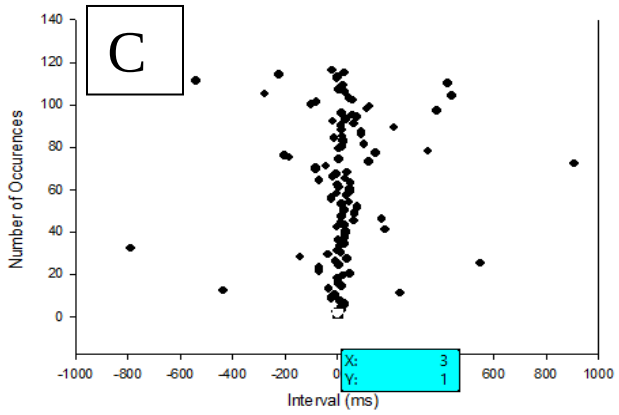

There is an overlap in the mEPSP recordings and GCaMP6 recordings (Figure 7, A&B).

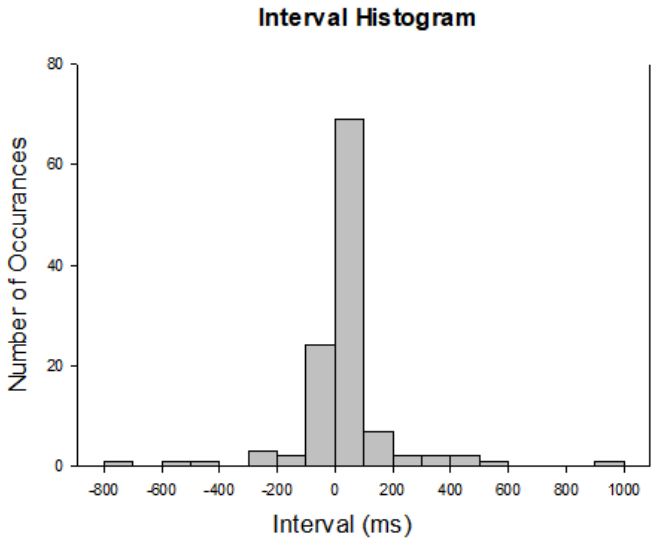

Figure 8. Shows a histogram of comparing the time difference in mEPSP and GCaMP6 events. There is a larger number of events that are recorded as positive, due to the mEPSP peaks being before the GCaMP6 peaks. This would be expected since the GCaMP signal is slower than the mEPSP (Supplemental Data).

Discussion

The obtained results indicate that at the *D. melanogaster* synapse we see missing excitatory post synaptic potentials (Figures 5, 6). When looking at the frequencies of GCaMP6 activation that is seen as fluorescence we have found that they do not match the frequencies of mEPSP recordings (Figure 4.). Simultaneous recording at one larva has found that there is a total of 141 mEPSPs while there is only 116 GCaMP6 flashes. Out of those 141 mEPSP recordings only 88 have been found to fall in the 116 flashes since there is overlap (multiple mEPSPs for one GCaMP6). This is possible since the rise time of the GCaMP6 sensor is 100-150ms (Chen et al., 2013). In the group of those 88 mEPSP recordings, 17 GCaMP6 events had intervals greater than 200ms (both positive and negative). These could be considered missing minis (Supplemental Data). The 53 mEPSP recordings that do not have a GCaMP6 event tied to them could belong to the group coming from the Is terminal which was not imaged in this preparation used for simultaneous recording. Our preparation 2 (Figures 1-3) is the only one with Is together with Ib. We have used this Is to estimate the frequency of the whole terminal in preparations 1-12. The frequency we obtained from Is was 0.98335 Hz, while the Ib frequency was 1.016 Hz (Table 6). Using these numbers I hypothesize that the 53 mEPSPs come from the Is terminal in our simultaneous preparation.

Immediately following a 20 Hz stimulation of muscle fibers 5 and 6 you get depression in frequency of mEPSPs (Powers et al., 2017). As mentioned before the unpublished data suggests that there are missing minis due to the decrease in their frequency, while there is sustained frequency of GCaMP6 fluorescence. What the data from this thesis suggests, is that due to the low number of missing minis recorded from the simultaneous recording it could be possible that during the 20Hz stimulation there is an effect postsynaptically that acts as a feedback mechanism (Powers et al., 2017).

One possibility is that in the *D. melanogaster* NMJ a structure known as the sub-synaptic reticulum, a folded membrane on the postsynaptic side, acts as a regulator of these missing quanta (Nguyen & Steward, 2016). Since spontaneous release has been found to regulate synaptic homeostasis, such as the maintaining of the spines in the synapse through AMPA receptor activation (McKinney et al., 1999), and the SSR in the neuromuscular junction resembles spines from the CNS (Rheuben et al., 1999), it could be possible that it somehow regulates the mEPSP response.

Imaging of the terminal using regions of interest (ROI) around active zones has found that the optical events correlate with changes in post-synaptic potentials (Cichon et al., 2020; Melom et al., 2013). Our results indicate that imaging the whole terminal, and selecting the boutons individually, reveals missing minis even without stimulation.

References

1. Atwood, H. L., Govind, C. K., & Wu, C. F. (1993). Differential ultrastructure of synaptic terminals on ventral longitudinal abdominal muscles in Drosophila larvae. *Journal of Neurobiology*, *24*(8), 1008-1024.
2. Augustine, G. J., & Kasai, H. (2007). Bernard Katz, quantal transmitter release and the foundations of presynaptic physiology. *The Journal of Physiology*, *578*(Pt 3), 623.
3. Bernstein, J. (1912). Elektrobiologie, Braunschweig, Friedr. *Vieweg und Sohn*.
4. Brand, A. H., & Perrimon, N. (1993). Targeted gene expression as a means of altering cell fates and generating dominant phenotypes. *Development*, *118*(2), 401-415.
5. Brooks V. B. (1956). An intracellular study of the action of repetitive nerve volleys and of botulinum toxin on miniature end-plate potentials. *The Journal of Physiology*, *134*(2), 264–277. https://doi.org/10.1113/jphysiol.1956.sp005642
6. Chen, T. W., Wardill, T. J., Sun, Y., Pulver, S. R., Renninger, S. L., Baohan, A., Schreiter, E. R., Kerr, R. A., Orger, M. B., Jayaraman, V., Looger, L. L., Svoboda, K., & Kim, D. S. (2013). Ultrasensitive fluorescent proteins for imaging neuronal activity. *Nature*, *499*(7458), 295–300. https://doi.org/10.1038/nature12354
7. Cichon, J., Magrané, J., Shtridler, E., Chen, C., Sun, L., Yang, G., & Gan, W. B. (2020). Imaging neuronal activity in the central and peripheral nervous systems using new Thy1. 2-GCaMP6 transgenic mouse lines. *Journal of Neuroscience Methods*, *334*, 108535.
8. Couteaux, R., & Pecot-Dechavassine, M. (1970). Synaptic vesicles and pouches at the level of" active zones" of the neuromuscular junction. *Comptes rendus hebdomadaires des seances de l'Academie des sciences. Serie D: Sciences naturelles*, *271*(25), 2346.
9. Deák, F., Shin, O. H., Kavalali, E. T., & Südhof, T. C. (2006). Structural determinants of synaptobrevin 2 function in synaptic vesicle fusion. *Journal of Neuroscience*, *26*(25), 6668-6676.
10. Del Castillo, J., & Katz, B. (1954a). Changes in end-plate activity produced by pre-synaptic polarization. *The Journal of Physiology*, *124*(3), 586-604.
11. Del Castillo, J., & Katz, B. (1954b). Quantal components of the end-plate potential. The *Journal of Physiology*, *124*(3), 560-573.
12. De Robertis, E., & Franchi, C. M. (1956). Electron microscope observations on synaptic vesicles in synapses of the retinal rods and cones. *The Journal of biophysical and biochemical cytology*, *2*(3), 307–318. https://doi.org/10.1083/jcb.2.3.307
13. Diego, F., Reichinnek, S., Both, M., & Hamprecht, F. A. (2013, April). Automated identification of neuronal activity from calcium imaging by sparse dictionary learning. *In 2013 IEEE 10th International Symposium on Biomedical Imaging* (pp. 1058-1061). IEEE.
14. Du Bois-Reymond, E. (1849). *Untersuchungen uber thierische Elektricitat*.
15. Ehlers, M. D., Heine, M., Groc, L., Lee, M. C., & Choquet, D. (2007). Diffusional trapping of GluR1 AMPA receptors by input-specific synaptic activity. *Neuron*, *54*(3), 447-460.
16. Fatt, P., & Katz, B. (1952). Spontaneous subthreshold activity at motor nerve endings. The *Journal of Physiology*, *117*(1), 109-128.
17. Frank C. A. (2014). Homeostatic plasticity at the Drosophila neuromuscular junction. *Neuropharmacology*, 78, 63–74. https://doi.org/10.1016/j.neuropharm.2013.06.015
18. Frank, C. A., Kennedy, M. J., Goold, C. P., Marek, K. W., & Davis, G. W. (2006). Mechanisms underlying the rapid induction and sustained expression of synaptic homeostasis. *Neuron*, *52*(4), 663–677. https://doi.org/10.1016/j.neuron.2006.09.029

19. Furshpan, E. J. (1956). The effects of osmotic pressure changes on the spontaneous activity at motor nerve endings. *The Journal of Physiology*, *134*(3), 689.
20. Galvani, L. (1792). Aloysii Galvani De viribus electricitatis in motu musculari commentarius. *Apud Societatem Typographicam*.
21. Galvani, L. (1937). *Memorie ed esperimenti inediti: con la iconografia di lui e un saggio di bibliografia degli scritti; a cura del Comitato per la celebrazione del 2o centenario della nascita di L. Galvani ea spese della cassa di risparmio in Bologna nella ricorrenza del primo secolo dalla sua fondazione*. Licinio Cappelli. (Original work published 1782)
22. Greenspan, R. J., (2004). *Fly pushing: The theory and practice of Drosophila genetics* (2nd eds.) (pp. 1-14). Cold Spring Harbor Laboratory Press.
23. Groffen, A. J., Martens, S., Díez Arazola, R., Cornelisse, L. N., Lozovaya, N., de Jong, A. P., Goriounova, N. A., Habets, R. L., Takai, Y., Borst, J. G., Brose, N., McMahon, H. T., & Verhage, M. (2010). Doc2b is a high-affinity Ca2+ sensor for spontaneous neurotransmitter release. *Science (New York, N.Y.)*, *327*(5973), 1614–1618. https://doi.org/10.1126/science.1183765
24. Harlow, M. L., Ress, D., Stoschek, A., Marshall, R. M., & McMahan, U. J. (2001). The architecture of active zone material at the frog's neuromuscular junction. *Nature*, *409*(6819), 479-484.
25. Helmholtz, H. (1850). Note sur la vitesse de propagation de l'agent nerveux dans les nerfs rachidiens. *CR Acad Sci (Paris)*, *30*, 204-206.
26. Helmholtz, H. V. (1852). Messungen über Fortpflanzungsgeschwindigkeit der Reizung in den Nerven. *Archiv für Anatomie, Physiologie und wissenschaftliche Medicin*, 19, 199-216.
27. Jin, I., Puthanveettil, S., Udo, H., Karl, K., Kandel, E. R., & Hawkins, R. D. (2012). Spontaneous transmitter release is critical for the induction of long-term and intermediate-term facilitation in Aplysia. *Proceedings of the National Academy of Sciences of the United States of America*, *109*(23), 9131–9136. https://doi.org/10.1073/pnas.1206914109
28. Kaeser, P. S., & Regehr, W. G. (2014). Molecular mechanisms for synchronous, asynchronous, and spontaneous neurotransmitter release. *Annual review of physiology*, *76*, 333-363.
29. Leitz, J., & Kavalali, E. T. (2014). Fast retrieval and autonomous regulation of single spontaneously recycling synaptic vesicles. *eLife*, *3*, e03658. https://doi.org/10.7554/eLife.03658
30. Matteucci, C., & Savi, P. (1844). *Traité des phénomènes électro-physiologiques des animaux*. Fortin, Masson.
31. Maximov, A., Shin, O. H., Liu, X., & Südhof, T. C. (2007). Synaptotagmin-12, a synaptic vesicle phosphoprotein that modulates spontaneous neurotransmitter release. *The Journal of Cell Biology*, *176*(1), 113–124. https://doi.org/10.1083/jcb.200607021
32. McKinney, R. A., Capogna, M., Dürr, R., Gähwiler, B. H., & Thompson, S. M. (1999). Miniature synaptic events maintain dendritic spines via AMPA receptor activation. *Nature neuroscience*, *2*(1), 44-49.
33. Melom, J. E., Akbergenova, Y., Gavornik, J. P., & Littleton, J. T. (2013). Spontaneous and evoked release are independently regulated at individual active zones. *Journal of Neuroscience*, *33*(44), 17253-17263.
34. Murthy, V. N., Sejnowski, T. J., & Stevens, C. F. (1997). Heterogeneous release properties of visualized individual hippocampal synapses. *Neuron*, *18*(4), 599-612.

35. Nakai, J., Ohkura, M., & Imoto, K. (2001). A high signal-to-noise Ca 2+ probe composed of a single green fluorescent protein. *Nature Biotechnology*, *19*(2), 137-141.
36. Nguyen, C. T., & Stewart, B. A. (2016). The influence of postsynaptic structure on missing quanta at the Drosophila neuromuscular junction. *BMC neuroscience*, *17*(1), 53. https://doi.org/10.1186/s12868-016-0290-7
37. Peled, E. S., Newman, Z. L., & Isacoff, E. Y. (2014). Evoked and spontaneous transmission favored by distinct sets of synapses. *Current Biology*, *24*(5), 484-493.
38. Peron, S., Chen, T. W., & Svoboda, K. (2015a). Comprehensive imaging of cortical networks. *Current Opinion in Neurobiology*, *32*, 115-123.
39. Peron, S. P., Freeman, J., Iyer, V., Guo, C., & Svoboda, K. (2015b). A cellular resolution map of barrel cortex activity during tactile behavior. *Neuron*, *86*(3), 783-799.
40. Petersen, S. A., Fetter, R. D., Noordermeer, J. N., Goodman, C. S., & DiAntonio, A. (1997). Genetic analysis of glutamate receptors in Drosophila reveals a retrograde signal regulating presynaptic transmitter release. *Neuron*, *19*(6), 1237-1248.
41. Piccolino, M. (1998). Animal electricity and the birth of electrophysiology: the legacy of Luigi Galvani. *Brain Research ulletin*, *46*(5), 381-407.
42. Powers, A. S., Grizzaffi, J., & Lnenicka, G. A. (2017). Increased postsynaptic Ca2+ reduces mini frequency at the Drosophila larval NMJ. *Synapse*, *71*(5), e21971.
43. Purves, D., Augustine, G.J., Fitzpatrick, D., Katz, L.C., LaMantia, A.S., McNamara, J.O., & Williams S.M. (Eds.). (2001). *Neuroscience* (2nd ed.; Chapter 5, "Synaptic transmission"). Sunderland, MA: Sinauer Associates.
44. Ramakrishnan, N. A., Drescher, M. J., & Drescher, D. G. (2012). The SNARE complex in neuronal and sensory cells. *Molecular and Cellular Neuroscience*, *50*(1), 58-69.
45. Reiff, D. F., Ihring, A., Guerrero, G., Isacoff, E. Y., Joesch, M., Nakai, J., & Borst, A. (2005). In vivo performance of genetically encoded indicators of neural activity in flies. *The Journal of Neuroscience: The Official Journal of the Society for Neuroscience*, *25*(19), 4766–4778. https://doi.org/10.1523/JNEUROSCI.4900-04.2005
46. Rheuben, M. B., Yoshihara, M., & Kidokorot, Y. (1999). Ultrastructural correlates of neuromuscular junction development. *International Review of Neurobiology*, *43*, 69-92. Academic Press.
47. Sara, Y., Virmani, T., Deák, F., Liu, X., & Kavalali, E. T. (2005). An isolated pool of vesicles recycles at rest and drives spontaneous neurotransmission. *Neuron*, *45*(4), 563-573.
48. Schwiening, C. J. (2012). A brief historical perspective: Hodgkin and Huxley. *The Journal of Physiology*, *590*(11), 2571-2575.
49. Sellin L. C. (1981). The action of batulinum toxin at the neuromuscular junction. *Medical Biology*, *59*(1), 11–20.
50. Sutton, M. A., Ito, H. T., Cressy, P., Kempf, C., Woo, J. C., & Schuman, E. M. (2006). Miniature neurotransmission stabilizes synaptic function via tonic suppression of local dendritic protein synthesis. *Cell*, *125*(4), 785-799.
51. Südhof, T. C. (2012). The presynaptic active zone. *Neuron*, *75*(1), 11-25.
52. Tian, L., Hires, S. A., Mao, T., Huber, D., Chiappe, M. E., Chalasani, S. H., Petreanu, L., Akerboom, J., McKinney, S. A., Schreiter, E. R., Bargmann, C. I., Jayaraman, V., Svoboda, K., & Looger, L. L. (2009). Imaging neural activity in worms, flies and mice with improved GCaMP calcium indicators. *Nature Methods*, *6*(12), 875–881. https://doi.org/10.1038/nmeth.1398

53. Walrond, J. P., & Reese, T. S. (1985). Structure of axon terminals and active zones at synapses on lizard twitch and tonic muscle fibers. *Journal of Neuroscience, 5*(5), 1118-1131.

Supplemental Data

GCaMP6 time (ms)	mEPSP time (ms)	interval (ms)
551	548	3
1151	1157	-6
1601	1444	19
1601	1582	19
1801	1769	32
2151	2119	32
3201	3188	13
3801	3646	-22
3801	3669	-22
3851	3823	-9
4101	3860	241
4702	5138	-436
5202	5233	-31
5252	5424	19
5502	5495	7
5952	5911	5
5952	5947	5
6302	6301	1
6552	6528	24
7802	7753	49
8002	8070	-68
8002	8576	-68
8002	9895	-68
9903	10005	8
10553	11442	548
11653	11659	-6
12153	12113	40
12353	12495	-142
12503	12538	-35
12553	12801	15
12803	12885	2
14254	15044	-790
15054	15575	10
15604	15943	29
15954	16350	11
16354	17623	4
17655	17833	32

Supplemental Data Table. Shows the recorded times for GCaMP6 events and mEPSP events from the same animal. Column A. Shows times for GCaMP6 event times. All events except the yellow-highlighted events have mEPSP events that correspond to them within at least a 100ms. The events in yellow are therefore missing minis. Column B shows the mEPSP event times. The red text indicates that these mEPSP recordings had no corresponding GCaMP6 signal, and are possibly from the Is terminal boutons whose GCaMP6 events were not recorded. The events in blue were added later on, by going through the data as not to miss any points. Column C shows the intervals between GCaMP6 flashes and the closest mEPSP event. This data was graphed as a scatter plot to visualize the missing minis (Figure 5).

17655	17971	32
17656	18441	33
18005	18655	34
18155	19276	184
18655	21239	0
19305	21592	29
21255	22260	16
21656	23285	64
23456	23907	171
24156	24139	17
24206	24728	67
24206	26539	67
24756	27161	28
24806	27682	78
24806	27728	78
26557	27920	18
27207	28681	46
27707	28779	-21
27707	28808	-21
27957	28992	37
28807	29600	-1
28857	29806	49
28857	31526	49
29607	32123	7
29808	33319	2
29858	33488	52
31458	36250	-68
31558	38338	32
32108	38734	-15
32708	38903	-2
33358	40392	39
33408	40912	-80
33408	41703	-80
36209	42003	-41
37159	42192	909
38460	42407	122
38910	43151	7
40210	43499	-182
40710	44286	-202
41060	45161	148
41260	46157	348

41710	46740	7
42210	46883	18
42511	46974	104
44311	48796	25
46762	49942	22
46962	50295	-12
49962	50619	20
50713	50945	94
50713	51897	94
50963	52767	18
51163	52829	218
51913	53530	16
51963	54711	66
52813	55058	-16
53263	55937	33
56314	59045	76
60665	59180	61
61265	60604	17
61765	61212	384
65106	61248	115
65116	61381	125
65316	63631	-100
66466	63733	-78
67617	63951	59
69717	64535	47
71117	64991	439
74968	65416	-276
75418	65627	31
78019	67558	9
81770	69091	17
84171	69670	23
84571	69962	423
87291	70456	-540
87471	70678	1
93223	72232	2
95523	72685	-221
95773	72720	29
95837	74004	-19
	75244	
	75387	
	75562	

	76477	
	77549	
	78010	
	78237	
	79460	
	81300	
	81753	
	82490	
	84148	
	87831	
	87852	
	92757	
	93073	
	93221	
	93262	
	95744	
	95856	
	32710	
	56238	
	53230	
	66544	
	87470	